3. A Study on a Supercavitating Hydrofoil with Rounded Nose

Hajime YAMAGUCHI*, *Member* and Hiroharu KATO**, *Member*

(*From J.S.N.A. Japan, Vol. 149, June 1981*)

Summary

Linearized theories on a supercavitating hydrofoil are not suitable for the foil with rounded nose where a sheet cavity does not generate from the leading edge of the foil. The theoretical result gives a negative infinite pressure at the leading edge because of singularity.

Furuya proposed a new theoretical method to remove the singularity by applying the singular perturbation method. But it can not give a definite position of cavity tip for a given cavity end. Developing Furuya's theory, the authors propose a new iterative method in which the position of cavity tip agrees with the laminar separation point.

Cavitation experiment was made for a hydrofoil with parabolic section. The test result was modified to remove wall effects of tunnel, using a newly developed method by the authors.

The calculated results by the proposed theory agreed with the experimental results on the pressure distribution as well as the cavity shape.

1. Introduction

In a previous paper[1], the authors reported the measurement of variation of cavity length with cavitation number for partially cavitating hydrofoils and compared them with calculated results using a linearized theory. However, the agreement was not good for thick hydrofoils with large leading edge radius. One of the reason for this might be that the theoretical assumption, i.e. cavity generates from the leading edge of the hydrofoil, was not realistic. In this paper the authors mainly investigate how this assumption affects the discrepancy between theoretical and experimental results. The problem is complicated, however, when we treat partial cavitation theoretically with practical cavity flow model. As a first step, therefore, the case of supercavitation is treated in this paper.

For the supercavitating case with the assumption of two-dimensional, incompressive, inviscid and steady flow, Riabouchinsky model, re-entrant flow model, transient flow model, etc. have been proposed and applied to bodies with simple shape such as flat plate and wedge. Wu *et al.*[2] proposed functional iterative method for application of his transient flow model solution of flat plate[3] to supercavitating hydrofoil with arbitrary profile. To the authors' knowledge, however, only Furuya[4] succeeded in applying this method to the hydrofoil with rounded nose. He performed calculations for a supercavitating flow with infinite cavity around a parabolic hydrofoil, but the calculation method is complicated and requires much time to compute. Thus the problem of supercavitating flows around hydrofoils with arbitrary profile is still very difficult to solve by present nonlinear theories.

* Graduate School, Department of Naval Architecture, The University of Tokyo

** Department of Naval Architecture, The University of Tokyo

On the other hand, if cavity tip does not coincide with the leading edge of the hydrofoil, linearized theory gives negative infinite pressure at the leading edge because of the singularity there. Thus it can be said that although linearized theory is quite suitable for a hydrofoil with sharp nose where flow separates from the leading edge of the hydrofoil, it does not give realistic results for a hydrofoil with rounded nose where cavity does not generate from the leading edge.

Furuya[5] proposed a new theoretical method to remove the singularity by applying the singular perturbation method[6] where nonlinearity near the leading edge was considered. However, one shortcoming of this method is that the cavity tip position can be arbitrarily defined for a certain cavity end position and the cavitation number is variable depending on the cavity tip position. On the other hand, it has been confirmed by Arakeri's experiments[7),8)] that the position of cavity tip agrees well with laminar separation point. Thus in order to remove the shortcoming the authors propose a new iterative method where cavity tip position coincides with the laminar separation point calculated from surface velocity distribution using Furuya's method.

Experiments were performed for a hydrofoil having parabolic section in cavitation tunnel to verify the proposed method. Surface pressure distribution, cavity tip and end position and cavity shape for different cavitation numbers were measured.

Assessment of wall effects of experimental channel is very important when supercavitation experiments are conducted. In this paper the wall effects are estimated based on the linearized singularity method proposed by Nishiyama[9], considering mirror image effect due to the upper and lower walls and experimental data are modified accordingly.

The adequacy of the proposed method is investigated by comparing the experimental results with the calculated ones.

2. Iterative calculation using Furuya's Method

2.1 Outline of Furuya's method

As mentioned in the foregoing, the essence of this method lies in the treatment of the nonlinearity near the leading edge. The assumption of cavitation number $\sigma \ll 1$, based on which Furuya developed his theory, is not adopted in this paper since it is not realistic when the cavity is relatively short. The following gives the outline of Furuya's theory.

(1) Assuming that the rounded nose of the hydrofoil is expressed by a parabola $y=\pm\varepsilon\sqrt{x}$ (ε: a small value), Cartesian coordinate system is defined as shown in Fig. 1. The nose profile is smoothly connected to arbitrary shapes given by $y=\varepsilon g(x)$ and $y=\varepsilon h(x)$ at points denoted by B and C, the trailing edge of the hydrofoil, cavity tip and end being denoted by D, A and E respectively. The respective x-coordinates of these points are denoted by Xb, Xc, 1, Xa and l. The uniform flow U is incident on the hydrofoil at a small angle α with respect to x-axis. On the pressure side of the hydrofoil the cavity is assumed to generate from the point D. The perturbation expansions for the velocity components in the x- and y-direction u and v are obtained as follows,

$$\frac{u}{U_c}=1+\varepsilon u_1+\varepsilon^2 u_2+\varepsilon^3 u_3+\cdots \qquad (1)$$

$$\frac{v}{U_c}=\varepsilon v_1+\varepsilon^2 v_2+\varepsilon^3 v_3+\cdots \qquad (2)$$

where U_c is the fluid velocity on the cavity

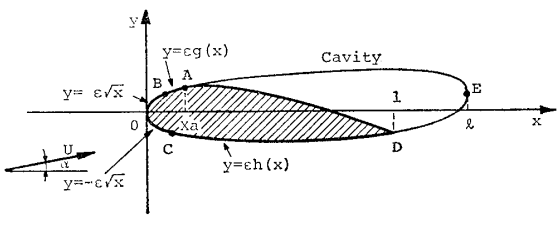

Fig. 1 Coordinate system for Furuya's method

expressed by the relation,

$$U_c = U\sqrt{1+\sigma} \qquad (3)$$

obtained from the Bernoulli equation.

(2) Introducing eqs. (1) and (2) into the boundary condition, i.e. "pressure is constant on the cavity surface and flow direction is parallel to the surface on the wetted portion of the hydrofoil", equations for u_1 and v_1 are obtained by comparing the terms of ε. The solution of u_1 and v_1 as obtained from these equations contain two unknown parameters besides σ. These are determined, however, from the condition of the uniform flow velocity at infinity and cavity closure condition. In this way the velocity distribution on the cavity and hydrofoil is obtained to the first order of ε, being called the outer solution. This solution has $x^{-1/2}$ singularity at the leading edge. Thus the inner region, where local nonlinear solution is necessary to remove the singularity, is the region given by $x=O(\varepsilon^2)$.

(3) Inner variables X and Y given by $X=x/\varepsilon^2$ and $Y=y/\varepsilon^2$ are next introduced, the parabolic nose $y=\pm\varepsilon\sqrt{x}$ being expressed by $Y=\pm\sqrt{X}$. The surface velocity in the inner region, which is called the inner solution, is derived for following two cases respectively, namely, the critical case where cavity tip is within the inner region and the regular case where it is not. This solution has two unknown parameters which are obtained by matching the outer solution as follows.

(4) According to "asymptotic matching principle" in singular perturbation method[6], the outer solution is expanded in terms of x the order of which is ε^2, making $Xa=O(1)$ in the regular case or $Xa=O(\varepsilon^2)$ in the critical case, and the inner solution in terms of x the order of which is 1. The unknown parameters are then adjusted so that the solutions match each other to the same order of ε.

(5) Uniformly valid solution of surface velocity is obtained by adding the inner and outer solution and subtracting the common part, which is used in above matching procedure.

In this way, the velocity distribution which is more realistic near the leading edge of the hydrofoil is obtained and this can be converted into the pressure distribution, using the Bernoulli equation. In this method, however, the cavity tip position is defined arbitrarily for a certain cavity end position and the solution is variable depending on the cavity tip position. In order to improve this shortcoming, the cavity tip position is defined with reference to the boundary layer on cavitating hydrofoil as follows.

2.2 Relation between laminar separation point and cavity tip position

As mentioned in the Introduction, it has been confirmed by Arakeri[7),8)], Casey[10)] that the cavity tip position coincides with the laminar separation point. Such phenomenon can be explained as follows.

Sufficient low pressure and residence time are necessary at the same time for a tiny gas nucleus in water to grow and become a cavity. Therefore, if the time taken for a nucleus to pass through the low pressure region upstream of the laminar separation point is very short, visible cavitation will not occur. On the other hand, if nuclei are trapped in the laminar separation bubble under ideal condition for growth, i.e. long residence time due to recirculation within the bubble and low pressure, they will form a sheet cavity, which is attached to the body surface. In order to reconfirm this phenomenon, the authors measured the surface velocity distribution on axisymmetric body in cavitating condition and compared the cavity tip position with calculated laminar separation point. Experiments were performed in the T.E. type cavitation tunnel[11)], using the hemispherical headform[11)] with the nose in the form of a hemisphere of diameter (D) 30 mm and smooth-

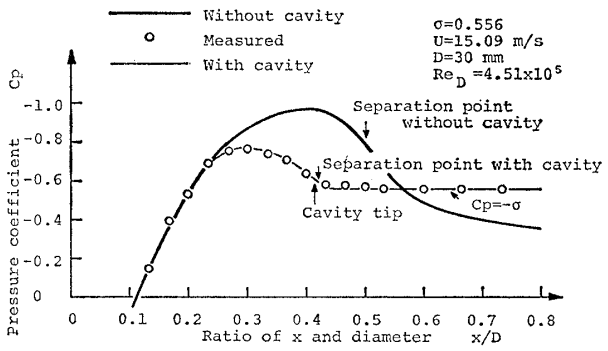

Fig. 2 Pressure distribution, separation point and cavity tip on hemispherical headform

ened to cylindrical form at the after end. Velocity on the body and cavity surface was measured by Laser Doppler Velocimeter and converted into pressure coefficient C_p, using the Bernoulli equation. One example of the experimental results is shown in Fig. 2 where x is the axial distance from the leading edge of the test body. The pressure distribution with cavity denoted by the fine line is different from that without cavity as shown by the thick line. The cavity tip position is upstream by about $0.09D$ from the laminar separation point without cavity[12]. However, calculated laminar separation point agrees with the cavity tip position. This fact represents that flow configuration is changed and laminar separation point is moved due to the occurrence of cavity. Moreover, these results show that the pressure on cavity agrees nearly with the vapour pressure of water, i.e. $C_p = -\sigma$, and there is a region upstream of the cavity tip where the pressure on body surface is lower than the vapour pressure of water, i.e. $C_p < -\sigma$.

2.3 Iterative method

As descrived above, it is evident that the cavity tip position coincides with the laminar separation point and can be estimated from the calculation considering the change of pressure distribution due to the occurrence of cavitation. The authors propose here an

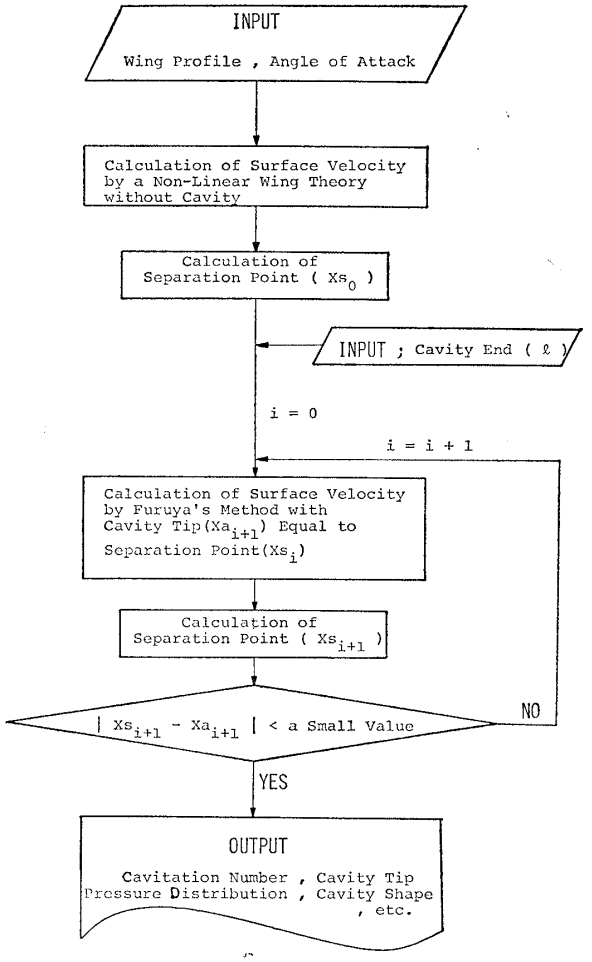

Fig. 3 Flow chart of iterative calculation to fix a unique position of cavity tip

iterative scheme of calculation as shown in Fig. 3 where the cavity tip is made to coincide with the laminar separation point calculated from the surface velocity distribution derived from Furuya's method. In this way, cavity tip position, cavitation number, cavity shape, pressure distribution, etc. are defined uniquely for a certain cavity end position.

2.4 Convergence of cavity tip

The authors investigated the convergence of cavity tip position Xa in the iterative calculation for the parabolic hydrofoil whose section is defined by $y = \pm 0.15\sqrt{x}$. The laminar separation point without cavity, Xs_0, which is taken to be the initial value of Xa, can not be obtained from calculation for this hydrofoil

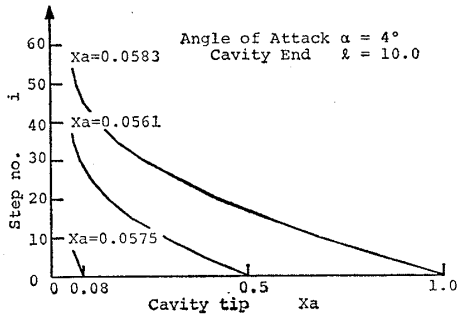

Fig. 4 Convergence of cavity tip on parabolic hydrofoil

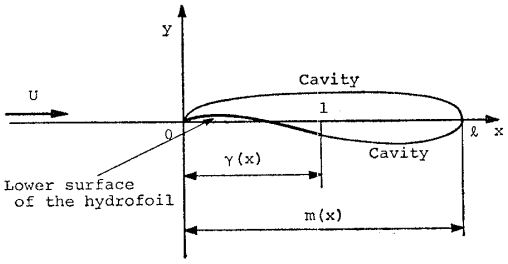

Fig. 5 Coordinate system for Nishiyama's method

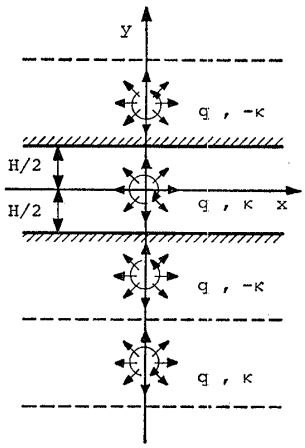

Fig. 6 Coordinate system of point source or point vortex in the middle of channel

since actual velocity distribution can not be obtained by potential flow calculation. Therefore, the authors investigated the convergence for three initial values of X_a, being taken to be 0.08, 0.5 and 1.0, and two angles of attack α, being taken to be 2° and 4°, respectively. As an example the result with $\alpha=4°$ and cavity and position $l=10.0$ is shown in Fig. 4. Although many iterations are required for some initial values to converge, all final values are nearly constant. In the case of $\alpha=2°$, all initial values converged to the trailing edge of the hydrofoil, i.e. $Xa=1.0$, and convergence was obtained after only four or five iterations at the most. The laminar separation point was computed by Thwaites' method, using the empirical constants as modified by Curle and Skan[13].

3. Investigation on wall effects

Effects of tunnel wall play an important role when supercavitation experiments are conducted in cavitation tunnel. In this paper the wall effects are estimated quantitatively, based on the linearized singularity method proposed by Nishiyama[9]. An outline of this method is given below.

(1) The x-axis is taken to be parallel to uniform flow U, the origin being at the leading edge of the hydrofoil where cavity generates, as shown in Fig. 5. The perturbation flow field is obtained in terms of the vortex distribution $\gamma(x)$ (which is positive in clockwise direction) and the source distribution $m(x)$ on x-axis representing the cavity and hydrofoil.

(2) Introducing linearized constant pressure condition on cavity and tangential flow condition on wetted portion of hydrofoil, integral equations for γ and m are obtained.

(3) Considering the nature of convergence and that of the singularities due to linearization, the singularity distribution γ and m are expressed in series form.

(4) Introducing cavity closure condition and satisfying the boundary conditions at some control points on x-axis, linear equations for coefficients of γ and m are obtained from the integral equations.

At first let the case where a point source q or a point vortex κ is situated at the origin

between two parallel walls at $y=\pm H/2$, H being the distance between the upper and lower walls, as shown in Fig. 6, be considered.

Introducing the complex variable

$$z=x+iy \tag{4}$$

and the complex velocity

$$w=u-iv \tag{5}$$

the complex velocity at point z due to the point source q or the point vortex κ is obtained respectively as

$$w_q=u_q-iv_q=\frac{q}{2H}\coth\left(\frac{\pi}{H}z\right) \tag{6}$$

$$w_\kappa=u_\kappa-iv_\kappa=-\frac{\kappa}{2iH}\frac{1}{\sinh\left(\frac{\pi}{H}z\right)} \tag{7}$$

by replacing the walls by infinite row of images at $y=\pm H, \pm 2H, \pm 3H, \ldots$[14]. Therefore, velocity induced only by the images of source q or vortex κ is obtained by subtracting $q/2\pi z$ and $-\kappa/2\pi iz$ from eqs. (6) and (7) respectively. Based on these two equations, the velocity induced by source and vortex distribution on x-axis is obtained and substituted in equations for the boundary conditions to obtain a new set of simultaneous linear equations.

Fig. 7 shows the relation between σ_H/σ and H/l where σ_H, σ, H and l are cavitation number with and without wall, distance between the upper and lower walls and cavity end position respectively. The solid line denotes the results for the parabolic hydrofoil and the chain dotted line that for the flat plate. Each line is independent of angle of attack. From the plot it can be said that cavitation number in presence of wall is larger for the same l or, in other words, l in presence of wall is larger for the same cavitation number, and the wall effect increases sharply as H/l become shorter and shorter. Fig. 7 also shows the result of partially cavitating case calculated in a similar manner[14]. This curve shows result similar to that of the supercavitating case, but the abscissa in this case is not H/l but H/C (C is the chord length of the hydrofoil).

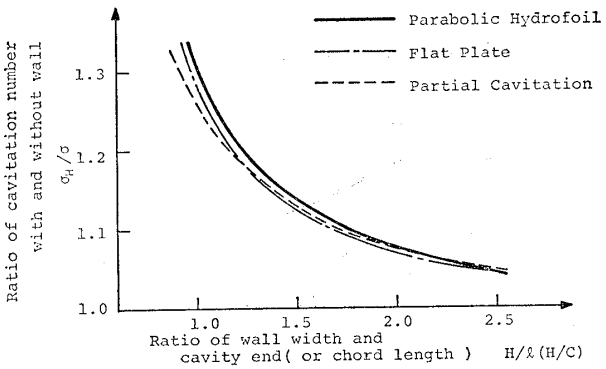

Fig. 7 Wall effect on cavitation number

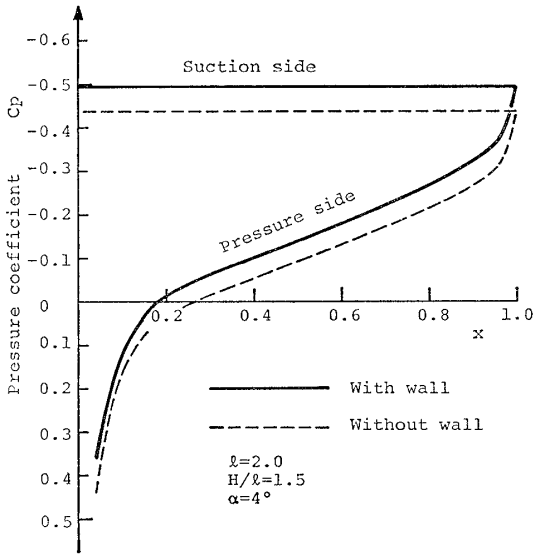

Fig. 8 Wall effect on pressure distribution of parabolic hydrofoil

Fig. 8 shows pressure distribution on the parabolic hydrofoil in presence of wall ($H/l=1.5$) and in absence of it for the case of $l=2.0$ and $\alpha=4°$. In presence of wall the pressure is lower in general but the lift is slightly larger.

As far as cavity shape is concerned, if the cavity ends are same, the effect of wall on cavity shape is so small that it is difficult to illustrate these effects through graphical plot.

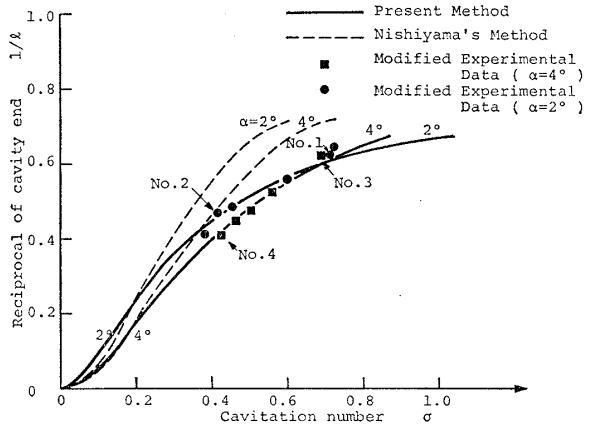

Fig. 9 Variation of cavity end with cavitation number

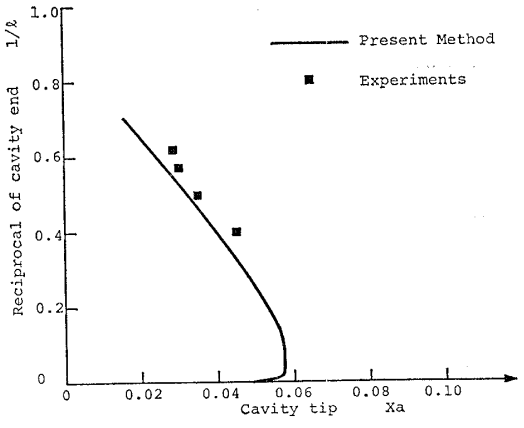

Fig. 10 Variation of cavity tip with cavity end

4. Comparison between experimental and calculated results

In order to verify the calculation method proposed in section **2**, experiments were performed for the parabolic hydrofoil. Cavity tip and end position, cavity shape and surface pressure distribution in cavitating condition were measured. The experiments were performed at the high speed cavitation tunnel of the Department of Naval Architecture, University of Tokyo. The test section was 120 mm in height and 25 mm in width. The chord length and span width of the model foil were 40 mm and 25 mm respectively. Experiments are performed at a uniform velocity of 25 m/s and for angles of attack of 2° and 4°.

Fig. 9 shows the variation of the reciprocal of cavity end position ($1/l$) with cavitation number. These experimental values were modified using the solid curve in Fig. 7. The experimental value of cavity end position is the mean value of about 35 photographs taken at the same condition. The calculated results of Nishiyama's method are also shown in Fig. 9, and the results of the present method agree well with the experimental ones.

Fig. 10 shows the variation of cavity tip position X_a with $1/l$, the angle of attack being 4°. Regarding cavity tip position also, the calculated result agrees well with the experimental results. With $\alpha=2°$, both experimental and calculated results showed $Xa=1$, i.e. the cavity generated from the trailing edge.

Fig. 11 shows the comparison of cavity shapes. In figures No. 1 through 4, the cavity end position for calculation is taken to be same as that obtained from the experiment marked by the same No. in Fig. 9, and in figure No. 5 it is assumed to be equal to 3.500 since the experimental cavity end position existed downstream of the observation window. The calculated results of Nishiyama's method are also shown in No. 2 and 4, where σ_e is cavitation number of experiment corrected for wall effects, σ_t is cavitation number of the present method, and σ_l is that of Nishiyama's method. Although from Nishiyama's method the cavity shapes are estimated to be thicker than those observed, the calculated cavity shapes of the present method agree well with the experimental ones except in the neighborhood of cavity end. Moreover, in comparison of Nishiyama's method cavitation number as calculated by the present method is closer to that of experiment, as is evident from Fig. 9.

Fig. 12 shows the comparison of pressure distribution at experiment points of No. 1 and 4 in Fig. 9 and No. 5 in Fig. 11. Similar

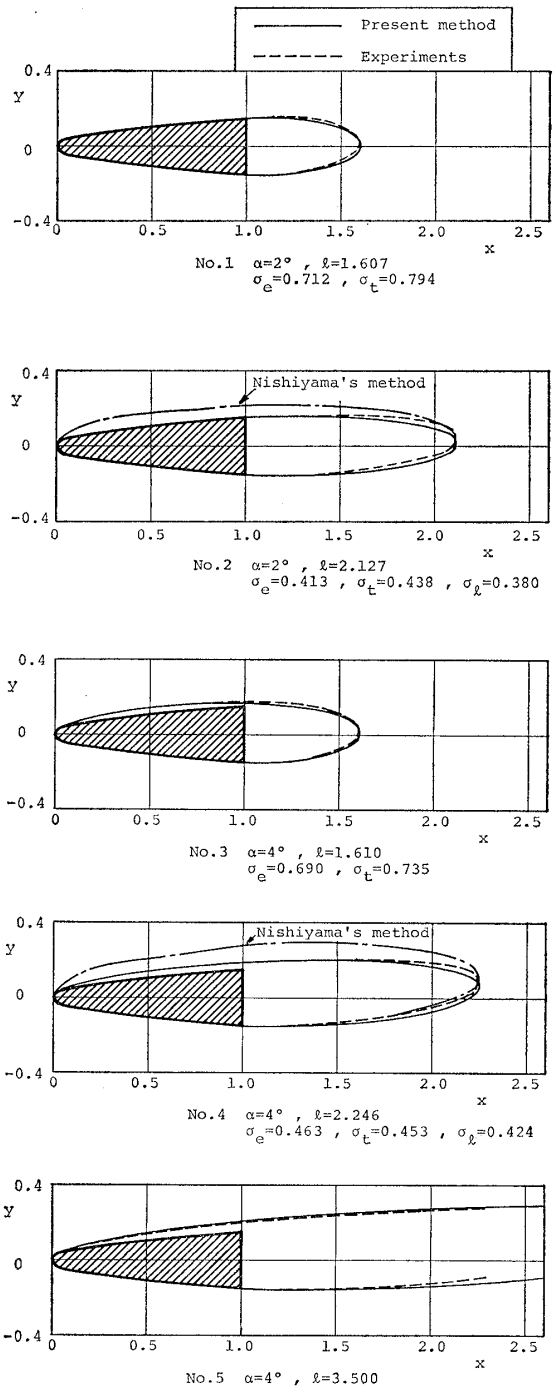

Fig. 11 Comparison of cavity shapes

to Fig. 2, the experimental values are shown in pressure coefficient C_p values which are calculated from the surface velocity distribution measured by Laser Doppler Velocimeter. Although direct comparison between the calculated and experimental results cannot be made because of considerable wall effects on pressure distribution as mentioned before, both seem to be in good agreement over a relatively wide region. It is also confirmed that similar to the case of axisymmetric body, there are regions upstream of the cavity tip where the pressure is lower than the vapour pressure.

5. Concluding remarks

A new computation scheme for a supercavitating hydrofoil with rounded nose where cavity does not generate from the leading edge of the hydrofoil is proposed, combining Furuya's method and calculation of laminar separation point.

In order to verify the proposed method, cavity tip and end position, cavity shape and surface pressure distribution for the hydrofoil with parabolic section were measured. The calculated results are found to be in good agreement with the experimental ones corrected for wall effects. It is clear from this that when a sheet type cavitation around a hydrofoil with large leading edge radius is considered, the fact that cavity tip does not coincide with the leading edge of the hydrofoil should be taken into account. Although only a supercavitating case has been treated in this paper, it is also possible to apply Furuya's method to a partially cavitating case[14]. With minor adjustments of problems in numerical calculation, the present proposed method can also be applied to a partially cavitating flow.

Furthermore, in order to investigate the relation between cavity tip and laminar separation point, the pressure distribution on a axisymmetric body in cavitating condition were measured, and the following conclusions were obtained.

(1) The laminar separation point calculated from the measured pressure distribution is very close to the cavity tip position.

(2) Regions with pressure below vapour pressure exist upstream of the cavity tip

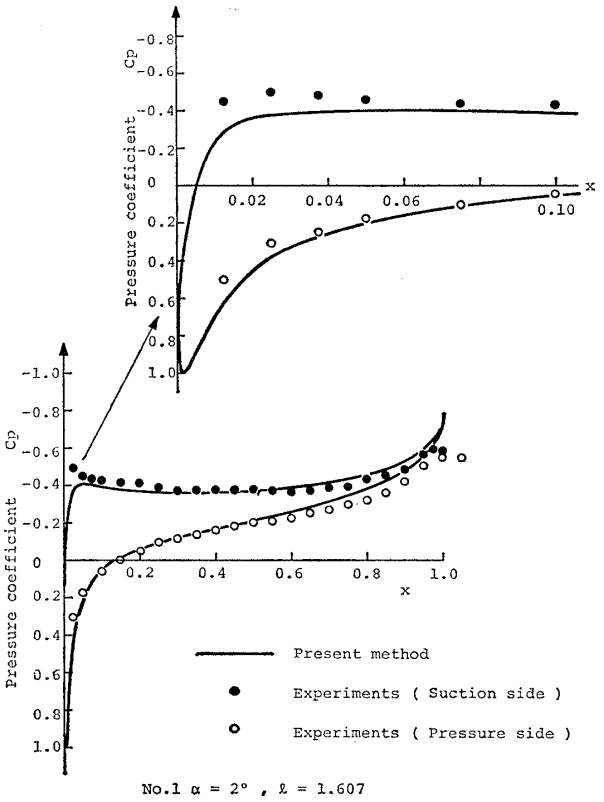

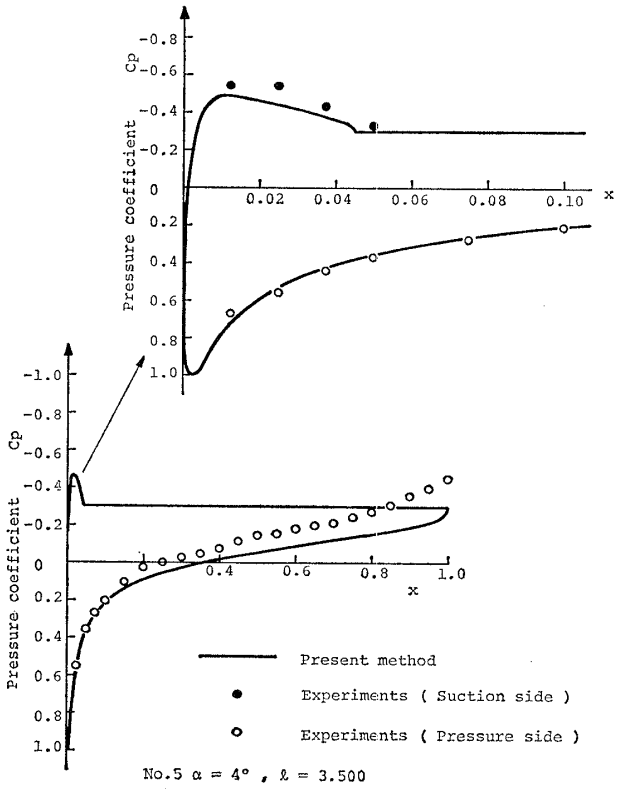

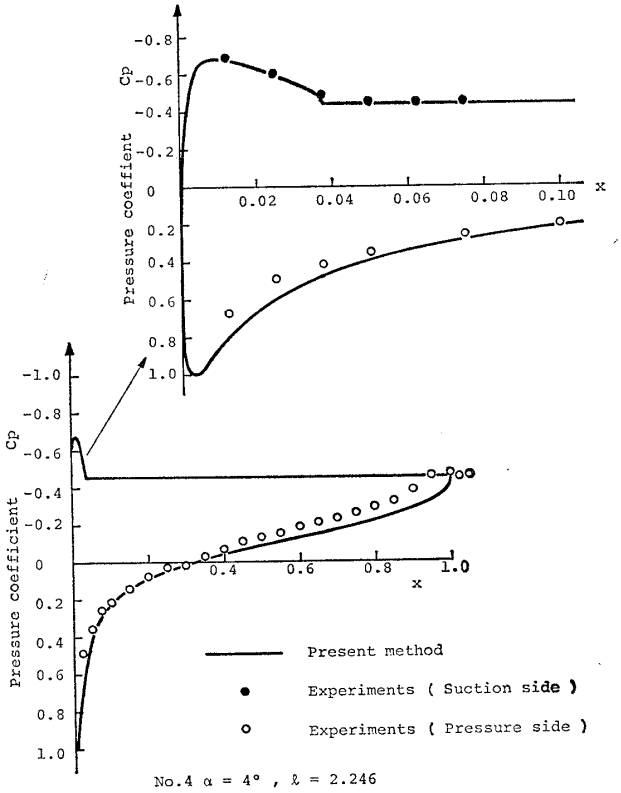

Fig. 12 Comparison of pressure distributions

(3) The cavity tip position and the laminar separation point in cavitating condition is different from the laminar separation point in non-cavitating condition.

(4) The pressure within the cavity is very close to the vapour pressure of water.

Moreover, in order to estimate the wall effects quantitatively, the calculation based on Nishiyama's method was performed, considering the mirror image effect due to the walls, the results of which are summarized as follows.

(1) The cavity in presence of walls is longer at the same cavitation number than the one in absence of these, but it can be converted into the one in absence of walls by the proposed method.

(2) Cavity shapes are not affected by walls if cavity ends are same. On the other hand, in presence of walls pressure distributions get modified and the lift is increased.

In the end, the authors would like to thank the staff of high speed hydrodynamic laboratory, Department of Naval Architecture, University of Tokyo in conducting the experiments. Especially the authors express their gratitude to M. Maeda for his helpful advice. The old HITAC 8800/8700 system at the Computer Center, University of Tokyo was used for the calculations in this paper.

References

1) Y. IZUMIDA *et al.*: The Cavitation Characteristics of Two-dimensional Hydrofoils, J. Soc. Naval Arch. Japan, Vol. 146 (1979), pp. 82–92, (in Japanese).
2) Y. T. WU and D. P. WANG: A Wake Model for Free-streamline Flow Theory Part 2. Cavity Flows past Obstacles of Arbitrary Profile, J. Fluid Mech., Vol. 18 (1963), pp. 65–93.
3) Y. T. WU: A Wake Model for Free-streamline Flow Theory Part 1. Fully and Partially Developed Wake Flows and Cavity Flows past an Oblique Flat Plate, J. Fluid Mech., Vol. 13 (1961), pp. 161–181.
4) O. FURUYA: Numerical Computations of Supercavitating Hydrofoils of Parabolic Shape with Wu and Wang's Exact Method, Office of Naval Research Department of the Navy Report No. E79A.15(1973).
5) O. FURUYA: A Singular Perturbation Method of Calculating the Behavior of Supercavitating Hydrofoils with Rounded Noses, Office of Naval Research Department of the Navy Report No. E79A.14(1972).
6) M. van DYKE: *Perturbation Methods in Fluid Mechanics,* ACADEMIC PRESS (1964), pp. 45–120.
7) V. H. ARAKERI and A. J. ACOSTA: Viscous Effects in the Inception of Cavitation on Axisymmetric Bodies, J. Fluid Engineering, Trans. of ASME, Vol. 95 (1973), pp. 519–527.
8) V. H. ARAKERI: Viscous Effects on the Position of Cavitation Separation from Smooth Bodies, J. Fluid Mech., Vol. 68 (1975), pp. 779–799.
9) T. NISHIYAMA: Calculation of Supercavitating Hydrofoils by Singularity Method, Trans. of JSME (part 2), Vol. 35, No. 277 (1969), pp. 1895–1902, (in Japanese).
10) M. V. CASEY: The Inception of Attached Cavitation from Laminar Separation Bubbles on Hydrofoils, Conference on Cavitation, Edinburgh (1974), pp. 9–16.
11) Y. KODAMA *et al.*: Study on Cavitation Inception (1st report), J. Soc. Naval Arch. Japan, Vol. 144 (1978), pp. 78–87.
12) Y. KODAMA *et al.*: Study on Cavitation Inception (2nd report)—Sheet Cavitation Inception—, J. Soc. Naval Arch. Japan, Vol. 146 (1979), pp. 93–100.
13) G. V. LACHMANN: *Boundary Layer and Flow Control–Volume 1–*, PERGAMON PRESS (1961), pp. 144–185.
14) H. YAMAGUCHI: Cavity Shape and Pressure Distribution on Hydrofoils with Sheet Type Cavitation, M. S. Thesis, University of Tokyo, Department of Naval Architecture (1980), (in Japanese).